

Reduction of the symmetry of a spin chain by external electric field and strain: Quantum effects

A. A. Zvyagin

*B.I. Verkin Institute for Low Temperature Physics and Engineering of the National Academy of Sciences of Ukraine,
Nauky Ave., 47, Kharkiv 61103, Ukraine;
Max-Planck Institut für Physik komplexer Systeme, Nöthnitzer Str., 38, D-01187 Dresden, Germany;
and V.N. Karazin Kharkiv National University, 4, Svoboda Sq., Kharkiv 61022, Ukraine*

 (Received 14 December 2021; revised 31 March 2022; accepted 31 March 2022; published 8 April 2022)

Quantum spin-1/2 system, in which spin, electric, and elastic subsystems are coupled, is studied analytically. We have shown that the external magnetic and electric field and strain, which reduce the symmetry, can affect many observable characteristics of the system. The analysis reveals how quantum critical values of the governing parameters can manifest themselves in the temperature behavior of those observables. Predicted effects can be useful for application in many fields of microelectronics.

DOI: [10.1103/PhysRevB.105.134409](https://doi.org/10.1103/PhysRevB.105.134409)

I. INTRODUCTION

Electro-magneto-elastic interaction attracts the attention of researchers. The main reason for such an attention is the practical use of that interaction. Namely, for instance, using the external magnetic field one can change their electric properties, or the application the external magnetic field can affect strains in the system, etc. Then the systems, in which the electro-magneto-elastic coupling is strong enough can be used as, e.g., switching devices, or the regulation units for memory storages in the modern microelectronics. Phononic control of magnetic properties [1,2], spintronics [3–5], magnetophononics [6], straintronics [7,8] are the prime examples of such an application. Piezoelectric systems are compounds, which can generate electric field from applied stress/strain, or vice versa, generate the strain as the reaction to the applied electric field [9]. Those systems can be used as ultrasonic detectors, ignition systems, sonar devices, or microphones. The possibility of the external field control of such devices with the Joule heat suppression implies achievement of ultralow power microelectronic devices, which is very important, especially at low energies. The most studied subjects, in which electro-magneto-elastic interaction manifests itself, are multiferroics, where, e.g., magnetic and ferroelectric order or both are present [10–16]. However, it is clear from general grounds that similar effects can exist in insulating spin systems without magnetic and ferroelectric ordering.

The nature of the electro-magneto-elastic coupling is the following. Ligands (nonmagnetic ions) surrounding magnetic ions determine the crystalline electric field, which acts on magnetic ions. This field, together with the spin-orbit interaction and the exchange coupling, defines the single ion magnetic anisotropy, or the magnetic anisotropy of the effective (indirect superexchange) interaction between spins in the spin system. Then strains of the elastic subsystem can change the distribution of ligands, changing the internal crystalline electric field. On the other hand, the external electric field also, as the crystalline electric field of ligands, acts on the orbital

moments of magnetic ions. The latter, in turn, due to the spin-orbit coupling, affect the single-ion spin anisotropy or the anisotropy of the indirect exchange coupling between spins. On the other hand, the external magnetic field changes the direction of spins, and affects via the spin-orbital coupling the orbital moments of ligands, changing, in turn, their positions via strains. Those changes also affect distribution of charges, yielding different electric characteristics. Symmetry of the system plays a crucial role in the determination of physical properties of such compounds. The change of the symmetry can yield transitions to novel physical phases with properties, different from the initial one.

It is important to study quantum many-body spin insulating system, in which interactions between spin, electric, and elastic subsystems can take place, to understand how that mechanism reveals itself there. Spin chain compounds can serve as the very good quantum many-body testing ground for the consideration of the interaction between electric, magnetic, and elastic subsystems. In those compounds the reduced dimensionality causes the enhancement of quantum and thermal fluctuations, which destroy magnetic ordering at nonzero temperatures [17]. However, the coupling between spins along the distinguished direction can be very strong, hence, those systems manifest quantum many-body effects. Also very important, spin-1/2 chains permit to obtain exact theoretical results [18], which give the opportunity to check them in comparison with the data of experiments in spin chain compounds.

Recently we have studied magnetic, electric, and elastic characteristics of the spin chain system coupled to the electric and elastic subsystem [19]. In that study we investigated the situation, in which the external electric field and strain do not change the symmetry of the system (to be precise, the symmetry was changed to the higher one only in one critical point). In the present paper we consider the qualitatively different case, in which the strain or the applied external electric field reduce, as a rule, the spin symmetry of the spin-1/2 chain system. Obviously, in spin-1/2 case there exists only interion magnetic anisotropy. We have calculated the renormalization

of the magnetic, electric, and elastic characteristics of the spin chain system caused by the symmetry-reducing coupling to the external electric field and strain. We show how quantum critical points, present in the system, with the coupling between spin, electric, and elastic subsystems determine the features of the low-temperature behavior of the mentioned characteristics.

II. HAMILTONIAN OF THE PROBLEM

The Hamiltonian of the considered orthorhombic spin chain compound, in which the spin subsystem is coupled to the electric and the elastic ones, can be written as [20,21]

$$\begin{aligned}
\mathcal{H} = & -H \sum_n S_n^z - I \sum_n (S_n^x S_{n+1}^x + S_n^y S_{n+1}^y) \\
& - J \sum_n (S_n^x S_{n+1}^x - S_n^y S_{n+1}^y) - J_z \sum_n S_n^z S_{n+1}^z \\
& + a_1 E \sum_n (S_n^x S_{n+1}^y - S_n^y S_{n+1}^x) + a_2 E \sum_n (S_n^x S_{n+1}^y \\
& + S_n^y S_{n+1}^x) + b_1 u \sum_n (S_n^x S_{n+1}^y - S_n^y S_{n+1}^x) \\
& + b_2 u \sum_n (S_n^x S_{n+1}^y + S_n^y S_{n+1}^x) + \frac{NC(u + u_0)^2}{2} \\
& + NeE(u + u_0) - \varepsilon \frac{NE^2}{8\pi}, \tag{1}
\end{aligned}$$

where $S_n^{x,y,z}$ are the operators of spin projections of the spins $1/2$ situated at the site n , H is the magnetic field H directed along the z axis (we use the units in which the product of the effective g -factor g and the Bohr magneton μ_B is equal to unity $g\mu_B = 1$), $I = (J_x + J_y)/2$, $J = (J_x - J_y)/2$, $J_{x,y,z}$ are the parameters of the magnetically anisotropic exchange interaction, (we consider mostly the case with $-|I| \leq J_z \leq |I|$; the most interesting effects are related to the aniferromagnetic spin-spin interactions). Then, $E \equiv E_y$ is the external electric field directed along the y axis (below we consider only the external electric field), ε is the related component of the electric permittivity, e is the related component of the piezoelectric modulus (do not confuse with the charge of the electron). Also, C is the elastic modulus (for this geometry it is C_{66}) (in what follows we call those components for simplicity just electric permittivity, piezoelectric modulus, and elastic modulus), u is the strain ($u \equiv u_{xy} - u_{xy0}$, and $u_0 \equiv u_{xy0}$ is the static strain), and $a_{1,2}$ and $b_{1,2}$ are the coefficients of the magneto-electric and magneto-elastic couplings, related to the exchange-antisymmetric and exchange-symmetric couplings, respectively (all issues are connected with the coordinate y). In highly symmetric crystals the elastic modules are related to the velocities of sound as $C = \rho v^2$, where ρ is the density of the crystal, and v is the velocity of sound. One often measures the velocities of sound to determine the absolute values of elastic modules and their relative changes as functions of, e.g., the temperature, the external fields, etc. [22]. On the other hand, the electric permittivity and the piezoelectric modulus can be also measured in magneto-electro-acoustic experiments [21,23,24]

In this contribution electric and elastic degrees of freedom of the system are studied as classical variables. In our consideration we limit ourselves with the longitudinal sound (for which the direction of the wave vector and polarization coincide). The form of the electro-magnetic and strain-spin and piezoelectric coupling in the Hamiltonian is the particular case of the general interactions between spin, electric, and elastic degrees of freedom $\sum_{m,n} \sum_{ipq} a_{ipq} E_i S_n^p S_m^q$, $\sum_{m,n} \sum_{ijpq} b_{ijpq} u_{ij} S_m^p S_n^q$, and $\sum_{ipq} e_{ipq} E_i u_{pq}$, where n, m numerate the lattice sites, and $i, j, p, q = x, y, z$ [20] with $a_{1,2}$, $b_{1,2}$, and e being the components of the tensors a_{ipq} , b_{ijpq} , and e_{ipq} . Here we use the form of magneto-electric and magneto-elastic couplings similar to [21] where the studied effects were observed in the magnetically ordered multiferroic. The considered effect is related to the orientation of the axes of the magnetic anisotropy of the spin-spin interaction in the chain, determined mostly by the distribution of non-magnetic ligands, surrounding magnetic ions, through which the indirect exchange between spins of magnetic ions is realized. The spin-orbit interaction together with the orientation of orbitals of ligands and magnetic ions affects the anisotropy of the interspin interactions in the chain, the key issue of the present study. For this direction of the electric field and related strains one deals with two kinds of the magneto-electric and magneto-elastic couplings, the exchange-symmetric and the exchange-antisymmetric ones (1). We see that strain- and electric field-induced magnetic anisotropy is lower than the original orthorhombic: They yield the monoclinic anisotropy. It principally differs this geometry from the one, studied in [19].

Suppose for simplicity that the chain is open (open boundary conditions). Then using the unitary transformation (rotation of all spins with respect to the axis z by the angle ψ) we can re-write the Hamiltonian (1) as

$$\begin{aligned}
\mathcal{H} = & \frac{NC(u + u_0)^2}{2} - I \sum_n (S_n^x S_{n+1}^x + S_n^y S_{n+1}^y) \\
& - J_1 \sum_n (S_n^x S_{n+1}^x - S_n^y S_{n+1}^y) - J_z \sum_n S_n^z S_{n+1}^z \\
& - H \sum_n S_n^z + NeE(u + u_0) + a_1 E \sum_n (S_n^x S_{n+1}^y \\
& - S_n^y S_{n+1}^x) + b_1 u \sum_n (S_n^x S_{n+1}^y - S_n^y S_{n+1}^x) - \varepsilon \frac{NE^2}{8\pi}, \tag{2}
\end{aligned}$$

where $J_1 = [J^2 + (a_2 E + b_2 u)^2]^{1/2}$ and $\tan 2\psi = -(a_2 E + b_2 u)/J$. Notice that the angle ψ does not enter the expression for the Hamiltonian for the open chain.

III. RENORMALIZATION OF THE MAIN CHARACTERISTICS

Then we perform the analysis similar to Ref. [19]. Consider the average value of the component of the spin quadrupole moment (here and below we deal only with the spin quadrupole moments) of the chain per site $Q_1 = (1/N) \sum_n \langle S_n^x S_{n+1}^y - S_n^y S_{n+1}^x \rangle$ (the brackets denote the averaging with the density matrix, and N is the length of the chain),

and χ_{Q1} , the component of the quadrupole susceptibility of the spin chain, related to Q_1 , and the average value of the other component of the spin quadrupole moment of the chain $Q_2 = (1/N) \sum_n (S_n^x S_{n+1}^x - S_n^y S_{n+1}^y)$, with χ_{Q2} , the component of the quadrupole susceptibility of the spin chain, related to Q_2 . From thermodynamics we know that $Q_1 = \partial F / \partial (a_1 E) = \partial F / \partial (b_1 u)$, where F is the free energy of the system per site, and $\chi_{Q1} = a_1^{-1} \partial Q_1 / \partial E = b_1^{-1} \partial Q_1 / \partial u$. On the other hand, it follows that $Q_2 = -\partial F / \partial J_1$ with $\partial Q_2 / \partial J_1 = \chi_{Q2}$. We can also use the obvious relations $\partial Q_1 / \partial E = a_1 \chi_{Q1}$, $\partial Q_1 / \partial u = b_1 \chi_{Q1}$, $\partial Q_2 / \partial E = [a_2(a_2 E + b_2 u) / J_1] \chi_{Q2}$, and $\partial Q_2 / \partial u = [b_2(a_2 E + b_2 u) / J_1] \chi_{Q2}$. It is easy to see that the component of the quadrupole moment Q_1 is nonzero only for $E_y \neq 0$ or $(u_{xy} - u_{xy0}) \neq 0$, (it is present in monoclinic systems), while Q_2 is nonzero in the absence of the electric field and strain (it is present in the orthorhombic system too).

From the elasticity theory [25] we define the component of the elastic deformation $\sigma \equiv \sigma_{xy}$, related to u_{xy} , as $\sigma = (\partial F / \partial u) = C(u + u_0) + eE + b_1 Q_1 - b_2(a_2 E + b_2 u) Q_2 / J_1$, and the definition of the piezoelectric modulus $e = (\partial \sigma / \partial E)$, see [20], it can be calculated

$$e_{\text{eff}} = e + a_1 b_1 \chi_{Q1} - a_2 b_2 f, \quad (3)$$

where

$$f = \frac{(a_2 E + b_2 u)^2 J_1 \chi_{Q2} + J^2 Q_2}{J_1^3}. \quad (4)$$

The definitions for the electric induction $D = -4\pi(\partial F / \partial E) = \varepsilon E - 4\pi e(u + u_0) - 4\pi a_1 Q_1 + 4\pi a_2(a_2 E + b_2 u) Q_2 / J_1$ and the electric permittivity $\varepsilon = \partial D / \partial E$ yield the effective permittivity

$$\varepsilon_{\text{eff}} = \varepsilon - 4\pi a_1^2 \chi_{Q1} + 4\pi a_2^2 f. \quad (5)$$

Finally, according to the elasticity theory [25] we have

$$\rho \frac{\partial^2 u}{\partial t^2} = \frac{d\sigma}{dx}. \quad (6)$$

The right-hand side of that equation can be transformed as

$$\begin{aligned} \frac{d\sigma}{dx} &= C \frac{\partial u}{\partial x} + e \frac{\partial E}{\partial x} + b_1 \left(b_1 \frac{\partial u}{\partial x} + a_1 \frac{\partial E}{\partial x} \right) \chi_{Q1} \\ &\quad - \frac{b_2 Q_2 J^2}{J_1^3} \left(a_2 \frac{\partial E}{\partial x} + b_2 \frac{\partial u}{\partial x} \right) \\ &\quad - \frac{b_2 (a_2 E + b_2 u)^2}{J_1^2} \left(b_2 \frac{\partial u}{\partial x} + a_2 \frac{\partial E}{\partial x} \right) \chi_{Q2}. \end{aligned} \quad (7)$$

Then we can calculate $\partial E / \partial x$ using the equation of the electric neutrality (we use here only the necessary component of the electric induction)

$$\begin{aligned} 0 = (\nabla \cdot D) &= \varepsilon \frac{\partial E}{\partial x} - 4\pi e \frac{\partial u}{\partial x} \\ &\quad - 4\pi a_1 \left(b_1 \frac{\partial u}{\partial x} + a_1 \frac{\partial E}{\partial x} \right) \chi_{Q1} \\ &\quad + \frac{4\pi a_2 (a_2 E + b_2 u)^2}{J_1^2} \left(b_2 \frac{\partial u}{\partial x} + a_2 \frac{\partial E}{\partial x} \right) \chi_{Q2} \\ &\quad + \frac{4\pi a_2 J^2 Q_2}{J_1^3} \left(a_2 \frac{\partial E}{\partial x} + b_2 \frac{\partial u}{\partial x} \right). \end{aligned} \quad (8)$$

The coefficient in the rewritten Eq. (6) in front of $\partial u / \partial x$ is the renormalized elastic modulus

$$C_{\text{eff}} = C + b_1^2 \chi_{Q1} - b_2^2 f + 4\pi \frac{e_{\text{eff}}^2}{\varepsilon_{\text{eff}}}. \quad (9)$$

For convenience we can introduce the relative changes of the electric permittivity $\Delta \varepsilon = (\varepsilon_{\text{eff}} - \varepsilon) / \varepsilon$, the piezoelectric modulus $\Delta e = (e_{\text{eff}} - e) / e$, and the elastic modulus $\Delta C = (C_{\text{eff}} - C) / C$.

We see that the renormalized electric permittivity, piezoelectric, and elastic module for the electric field directed along y axis and the strain u_{xy} , which reduce the symmetry of the system from the orthorhombic to the monoclinic, are determined by two (not by one component of the tensor of the quadrupole susceptibility, as for the the electric field E_x and the strain $u_{xx} - u_{yy}$, which keep the symmetry orthorhombic or enlarge the symmetry to the tetragonal one) [19], components of the quadrupole susceptibility, and on the component of the quadrupole moment itself. The effect of the exchange-antisymmetric coupling is determined by the component of the quadrupole susceptibility, similar to the previous case [19]. It is characteristic for the monoclinic symmetry, while the effect of the exchange-symmetric coupling is determined by the quadrupole susceptibility and the quadrupole moment itself, characteristic to the orthorhombic symmetry, in the combination f , in contrast to the previous case. Contributions from the exchange-antisymmetric and exchange-symmetric parts of the electric-quadrupole and strain-quadrupole couplings renormalize the effective electric permittivity, piezoelectric modulus, and elastic modulus in opposite ways, reducing or enlarging their values (at least formally, see below). The mentioned components of the quadrupole susceptibility and the quadrupole moment of the spin chain can be calculated as derivatives of the thermodynamic potential, the Helmholtz free energy F . Hence, in the framework of the Gibbs canonical ensemble, they do not depend on the eigenfunctions of the system. It is not so, when one calculates some other characteristics of the system, which cannot be expressed as the derivatives of the thermodynamic potential, e.g., correlation functions between non neighboring spins.

IV. SPECIAL CASES

To find the free energy F of the spin chain with the Hamiltonian (1) or (2), we can use the Jordan-Wigner transformation [26] connecting spin operators and operators of creation and destruction of spinless fermions. Using then the Fourier transformation we rewrite the Hamiltonian (2) as [27]

$$\begin{aligned} \mathcal{H} &= \frac{NC(u + u_0)^2}{2} - \varepsilon \frac{NE^2}{8\pi} + NeE(u + u_0) \\ &\quad - I_1 \left(\frac{Nh}{2} + \frac{N\Delta}{4} + \sum_k \left[(h - \cos(k - \phi)) a_k^\dagger a_k \right. \right. \\ &\quad \left. \left. - \frac{\gamma}{2} (a_{-k} a_k e^{-ik} + \text{H.c.}) - \frac{\Delta}{N} \cos(k) \rho_{-k} \rho_k \right] \right), \end{aligned} \quad (10)$$

where a_k^\dagger (a_k) creates (destroys) the fermion with the quasi-momentum k , $I_1 = [I^2 + (a_1 E + b_1 u)^2]^{1/2}$, $\Delta = J_z / I_1$, $\gamma =$

J_1/I_1 , $\tan \phi = (a_1 E + b_1 u)/I$, and $\rho_k = \sum_p a_{p+k}^\dagger a_p$. We see that Eq. (10) is the generalized lattice form of the Hamiltonian of the one-dimensional massive Thirring model [28], see also [29,30]. For the one-dimensional massive Thirring model the eigenvalues of the Hamiltonian can be written as [31–34]

$$\frac{E_T}{N} = \frac{C(u + u_0)^2}{2} - \varepsilon \frac{E^2}{8\pi} + eE(u + u_0) - \frac{I_z}{4} - \frac{I_1 h}{2} + \frac{I_1 \Delta}{N} \sum_{j=1}^M (h - |\gamma| \cosh \beta_j), \quad (11)$$

where the rapidities $\{\beta_j\}_{j=1}^M$ are determined as the solutions of the Bethe ansatz equations

$$N|\gamma| \sinh \beta_j = 2\pi A_j + \phi + 2 \sum_{\substack{k=1 \\ k \neq j}}^M \tan^{-1}[\Delta(\tan(\beta_j - \beta_k)/2)], \quad (12)$$

A_j are integers or half-integers, and M is the number of spins down. Solving the set of equations (12) with respect to β_j , and putting the solutions to (11) one gets eigenvalues of the one-dimensional massive Thirring Hamiltonian. The phase ϕ determines the finite-size corrections [35].

Let us define new more convenient parameters $a = |\gamma| \exp[\xi \Lambda/(\pi + \xi)]$, where $i\xi = \ln[(1 + i\Delta)/(1 - i\Delta)]$ is determined by the interaction J_z , and the parameter Λ is connected with the number of down spins via $(M/N) = (a\xi/\pi \sin(\xi)) \sinh[\pi \Lambda/(\pi + \xi)]$. Notice that for the noninteracting case $J_z = 0$ one gets $a = |\gamma|$. Then the ground state energy of the model per site can be written as

$$\begin{aligned} \frac{E_{Tg}}{N} = & \frac{Cu^2}{2} - H \left[\frac{1}{2} - \frac{a\xi}{\pi \sin(\xi)} \sinh \left(\frac{\pi \Lambda}{\pi + \xi} \right) \right] \\ & - \frac{I_1 a \xi}{2 \sin(\xi)} \left[\frac{1}{2\pi + \xi} \sinh \left(\frac{(2\pi + \xi)\Lambda}{\pi + \xi} \right) - \frac{J_z}{4} \right. \\ & \left. - \xi^{-1} \sinh \left(\frac{\xi \Lambda}{\pi + \xi} \right) \right] + eEu - \varepsilon \frac{E^2}{8\pi}. \end{aligned} \quad (13)$$

For example, at $H = 0$ we have $M = N/2$, which defines the value of $\Lambda = [(\pi + \xi)/\pi] \sinh^{-1}[\pi \sin(\xi)/2a\xi]$. Differentiation of the ground-state energy E_{Tg} with respect to J , E , or u yields the necessary values of $Q_{1,2}$ and $\chi_{Q1,2}$ for the considered model in the ground state as a function of H , E , and u . One can, using the developed technique of the thermal Bethe ansatz [18], construct nonlinear integral equations, which describe thermodynamics of the one-dimensional massive Thirring model. However it is impossible to obtain analytic solutions of those equations in the closed form (except of the limiting cases of low and high temperatures). The other two ways to take into account interactions between spinless fermions in (10) is to use [36] the Bethe ansatz solution for the XYZ spin chain [37] (known only for $H = 0$, however for the lattice case), or the Hartree-Fock-like approximation, which were used for the considered spin chain in the case of nonzero E_x and $u_{xx} - u_{yy}$ [19].

The situation is simplified for the case $J_z = 0$, for which the Hamiltonian (10) is the quadratic form of Fermi operators. Using the Bogoliubov transformation we obtain for the free

energy of the system per site

$$F = \frac{C(u + u_0)^2}{2} - \varepsilon \frac{E^2}{8\pi} + eE(u + u_0) - \frac{T}{N} \sum_k \ln [2 \cosh(\varepsilon_k/T)], \quad (14)$$

where T is the temperature (we use the units in which the Boltzmann constant is unity, $k_B = 1$), and

$$\begin{aligned} \varepsilon_k = & [a_1 E + (b_1 u)] \sin(k) \\ & + \sqrt{(H - I \cos(k))^2 + J_1^2 \sin^2(k)}. \end{aligned} \quad (15)$$

The expectation values of $Q_{1,2}$ and $\chi_{Q1,2}$, can be easily calculated from Eqs. (14) and (15),

$$\begin{aligned} Q_1 = & -(2N)^{-1} \sum_k \sin(k) \tanh \left(\frac{\varepsilon_k}{2T} \right), \\ \chi_{Q1} = & -(4NT)^{-1} \sum_k \frac{\sin^2(k)}{\cosh^2 \left(\frac{\varepsilon_k}{2T} \right)}, \\ Q_2 = & (2N)^{-1} \sum_k \frac{J_1 \sin^2(k) \tanh \left(\frac{\varepsilon_k}{2T} \right)}{\sqrt{(H - I \cos(k))^2 + J_1^2 \sin^2(k)}}, \\ \chi_{Q2} = & (4NT)^{-1} \sum_k \left[\frac{J_1^2 \sin^4(k)}{[(H - I \cos(k))^2 + J_1^2 \sin^2(k)]} \right. \\ & \times \cosh^{-2} \left(\frac{\varepsilon_k}{2T} \right) \\ & \left. + \frac{2T \sin^2(k)(H - I \cos(k))^2}{[(H - I \cos(k))^2 + J_1^2 \sin^2(k)]^{3/2}} \tanh \left(\frac{\varepsilon_k}{2T} \right) \right]. \end{aligned} \quad (16)$$

We see that the component of the quadrupole susceptibility related to the exchange-antisymmetric coupling, is negative, hence the total renormalization of the electric permittivity is positive, similar to the previously studied case [19]. It is easy to see that f is positive, hence there are two contributions, which determine the renormalization of the elastic modulus. The first one is the magneto-elastic contribution, which yields the softening of the modulus, and the other one, caused by the piezoelectricity, yields hardening of the elastic modulus.

V. ANALYSIS OF THE RESULTS

The low-temperature behavior of all thermodynamic characteristics of the spin chain is determined by quantum critical points (lines), governed by the magnetic field H and the electric field E , or the strain u .

Quantum critical points (lines), as usual for quantum chain systems, are determined by the dispersion law ε_k . It is easy to see that for $(a_1 E + b_1 u)^2 < J_1^2$ the dispersion law is gapped for all k except of the value of $H = H_{c1} = I$ at which the dispersion law is gapless at $k = 0$. On the other hand, the dispersion law is gapless for $(a_1 E + b_1 u)^2 \geq J_1^2$ and $H^2 \leq H_{c2}^2 = I^2 + (a_1 E + b_1 u)^2 - J_1^2$.

At $H = 0$ the quantum critical values (lines in the ground state E - u phase diagram) are determined from the equation

$$(a_1^2 - a_2^2)E_c^2 + (b_1^2 - b_2^2)u_c^2 + 2(a_1 b_1 - a_2 b_2)E_c u_c = J^2. \quad (17)$$

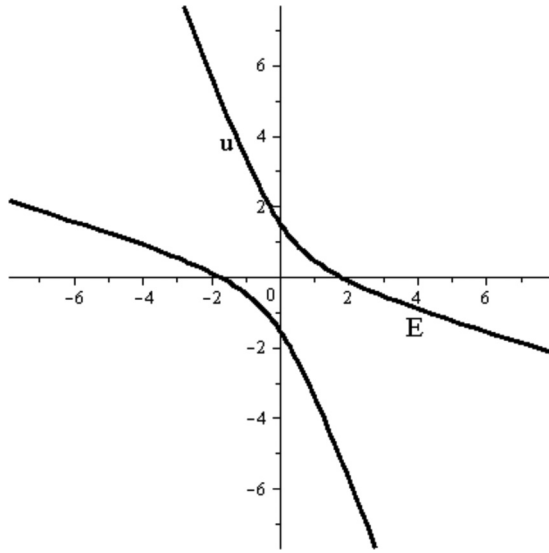


FIG. 1. The ground state E - u phase diagram of the spin chain system in the absence of the magnetic field for $J_z = 0$ in the nondegenerate case.

In the most degenerate trivial case $a_1 = a_2$ and $b_1 = b_2$ there are no critical values of the electric field and strain, and the dispersion law is gapped (except of the critical point $H = H_c$ at $k = 0$ for a nonzero magnetic field). In the less degenerate cases, e.g., if $a_1 = a_2 = a$ and $b_1 \neq b_2$, there is only one critical value (parabolic line in the ground state phase diagram electric field-strain) of the electric field

$$E_c = \frac{(b_1 + b_2)u_c^2 - J^2}{2au_c}, \quad (18)$$

and vice versa, if $b_1 = b_2 = b$ and $a_1 \neq a_2$, there is only one critical value (parabolic line in the ground-state phase diagram) of the strain

$$u_c = \frac{(a_1 + a_2)E_c^2 - J^2}{2bE_c}. \quad (19)$$

In the general case the critical line in the ground-state phase diagram electric field-strain is the rotated hyperbola, see Eq. (17). The ground state phase diagram is illustrated in Fig. 1: It corresponds to the case with $a_1^2 - a_2^2 > 0$ and $b_1^2 - b_2^2 > 0$, in which there exist the critical strain at zero electric field and the critical electric field at zero strain. Notice that at all those critical lines $H_{c1} = H_{c2}$. In the region of the phase diagram between two critical lines the dispersion law of spin excitations is gapped, in the other regions it is gapless.

There are only two quantum critical points of the model, governed by the magnetic field, namely H_{c1} , present in the gapped part of the E - u ground-state phase diagram, and H_{c2} , present in the gapless part. At the critical line of the E - u diagram both values are equal, $H_{c1} = H_{c2}$.

The standard way to see the influence of the critical point governed by the magnetic field H is to study the magnetic field dependence of the magnetic moment and the magnetic susceptibility. The z projection of the magnetic moment per

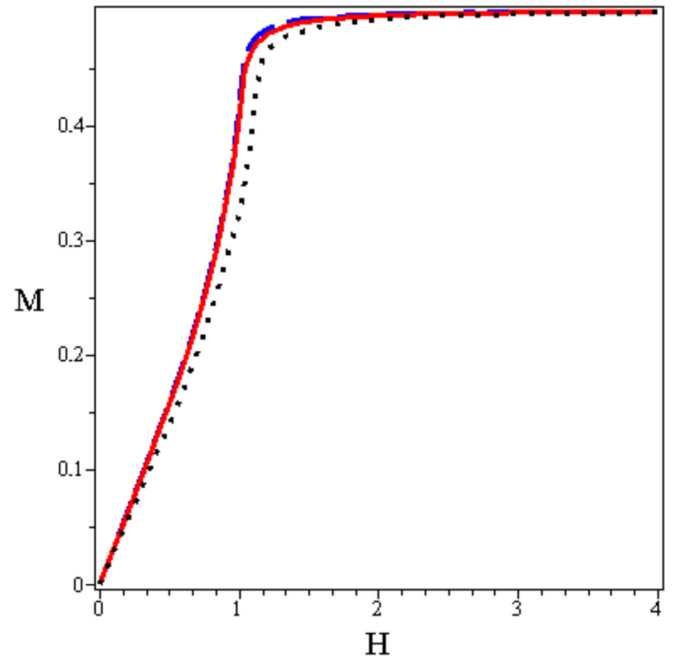


FIG. 2. Magnetic moment of the spin-1/2 chain with $I = 1$, $J = 0.3$, $J_z = 0$ for $T = 0.01$ and $a_1 = 1$, $a_2 = 0.5$ as a function of the external magnetic field H for the external electric field $E = 0$ (blue-dashed line), $E = E_c = 0.2\sqrt{3}$ (red-solid line), and $E = 0.7$ (black-dotted line).

site, which is equal to

$$M = \frac{1}{2N} \sum_k \frac{(H - I \cos k) \tanh\left(\frac{e_k}{2T}\right)}{\sqrt{(H - I \cos(k))^2 + J_1^2 \sin^2(k)}}, \quad (20)$$

as well as the magnetic susceptibility $\chi = \partial M / \partial H$, can be easily calculated. In the ground state the magnetic susceptibility manifests the logarithmic singularity at $H \rightarrow H_{c1}$ for the values of the electric field and strain, satisfying the relation $(a_1 E + b_1 u)^2 < J_1^2$, and the square root singularity at $H = H_{c2}$ for $(a_1 E + b_1 u)^2 > J_1^2$.

In what follows we consider the case $u = 0$ for simplicity, and investigate the effect of the electric field on the studied characteristics of the spin chain system. In that case there is only one value of the critical electric field $E_c = \pm J / \sqrt{a_1^2 - a_2^2}$. It is clear from the above that the effect of the strain can be considered in a similar way, with the obvious change $a_{1,2} E \rightarrow b_{1,2} u$, and with qualitatively similar behavior.

Figures 2 and 3 manifest the low-temperature ($T = 0.01$) magnetic field behavior of the magnetic moment and the magnetic susceptibility. In these figures and in what follows the following parameters are used: $I = 1$, $J = 0.3$, $a_1 = 1$, $a_2 = 0.5$, $b_1 = -1$, $b_2 = -0.5$, $e = 2$, $\varepsilon = 20$, and $C = 8.5$.

We see that at low temperatures the magnetic moment and the component of the magnetic susceptibility χ depend on the values of the external electric field (and strain) too. However, unlike the different direction of the electric field, see [19], the difference in the behavior of these magnetic characteristic is not so dramatic at the critical value of the electric field E_c . For instance, for the electric fields close to E_c , for nonzero

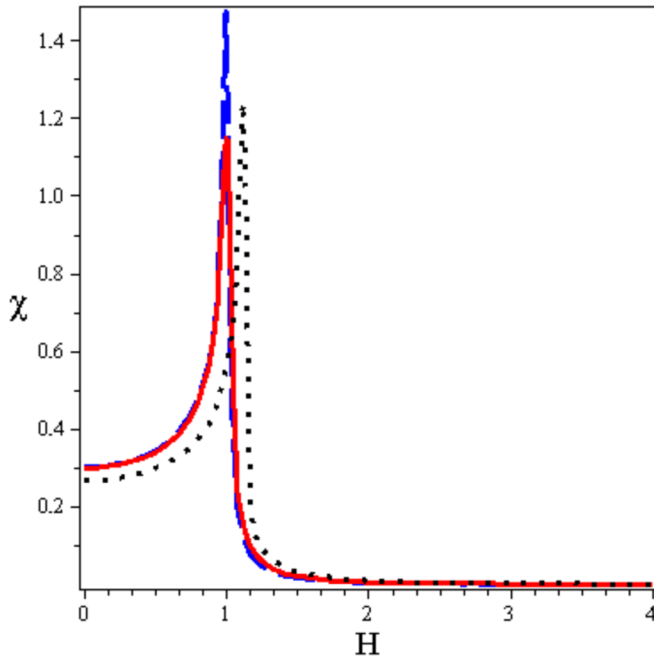


FIG. 3. Magnetic susceptibility for the spin-1/2 chain as a function of the external magnetic field H and various values of the external electric field E . The parameters and notations are the same as in Fig. 2.

temperature it is difficult to distinguish between the square-root and logarithmic singularities present in the ground state magnetic susceptibility.

Let us now illustrate the features of the quantum phase transitions in magneto-electric, magneto-elastic, and piezo-electric effects in the spin chain system.

First, let us examine the influence of the quantum critical point, governed by the magnetic field, on the calculated above relative changes of the piezoelectric modulus, electric permittivity and elastic modulus.

Fig. 4 manifests the temperature behavior of the piezoelectric modulus of the spin chain for various values of the magnetic field H . We see that in general the temperature behavior of $\Delta\epsilon$ manifests a plateau-like behavior at low temperatures, then it grows with T , reaches the maximum, and then it shows monotonic decay with the growth of the temperature. The piezoelectric modulus in general decreases with the growth of the applied magnetic field. The quantum critical point at $H = H_{c1}$ reveals itself in the absence of the low-temperature plateau.

Similar behavior is demonstrated by the electric permittivity, see Fig. 5. It is clear, because the formulas for the changes of the electric permittivity and the piezoelectric modulus are similar. Again, the external magnetic field yields the decrease of the electric permittivity of the system.

Finally, Fig. 6 shows the relative changes of the elastic modulus with temperature for various values of the external magnetic field.

We can see that at high temperatures the elastic modulus is softening with the decay of T , shows a minimum, and then, manifests the hardening at lower temperatures. At all values of the applied magnetic field except of the quantum critical value $H = H_c$ the elastic modulus shows small plateaux at

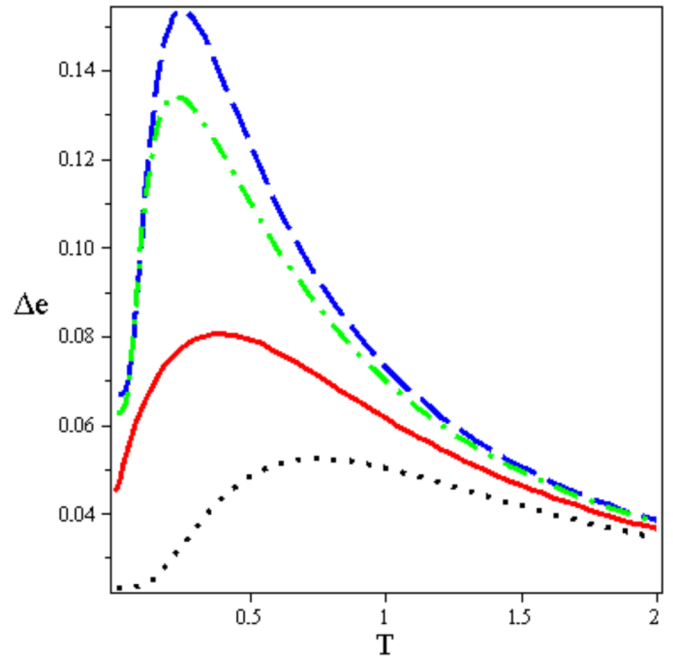


FIG. 4. The temperature dependence of the relative change of the piezoelectric modulus of the spin-1/2 chain for various values of the external magnetic field H . The parameters of the Hamiltonian are the same as in Fig. 2. $H = 0$ corresponds to the blue-dashed line; $H = 0.5$ is shown with the green-dashed-dotted line, $H = H_{c1} = 1$ is for the red solid line, and $H = 1.5$ is shown with the black-dotted line.

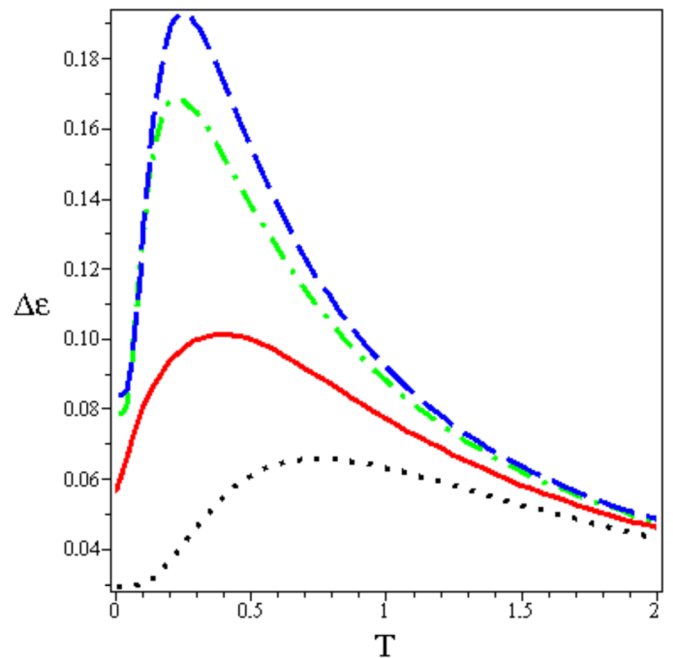


FIG. 5. The temperature dependence of the relative change of the electric permittivity of the spin-1/2 chain for various values of the external magnetic field H . The parameters of the Hamiltonian are the same as in Fig. 2. $H = 0$ corresponds to the blue-dashed line; $H = 0.5$ is shown with the green-dashed-dotted line, $H = H_{c1} = 1$ is for the red-solid line, $H = 1.5$ is for the black-dotted line.

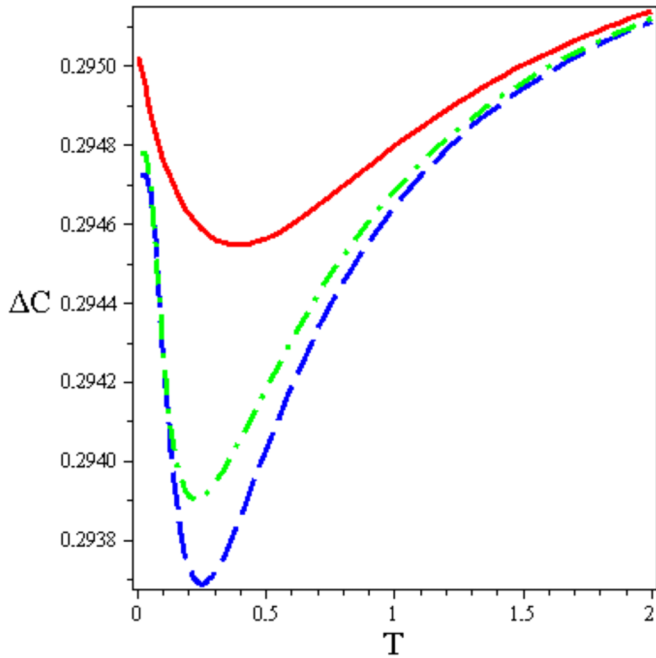


FIG. 6. The temperature dependence of the relative change of the elastic modulus of the spin-1/2 chain for various values of the external magnetic field H . The parameters of the Hamiltonian are the same as in Fig. 2. $H = 0$ corresponds to the blue-dashed line; $H = 0.5$ is shown with the green-dashed-dotted line, $H = H_{c1} = 1$ is for the red-solid line.

the lowest temperatures. The applied magnetic field yields the hardening of the elastic modulus.

Then we examine the influence of the quantum critical point, caused by the external electric field on the mentioned characteristics of the spin chain.

Again, the temperature behavior of the piezoelectric modulus, see Fig. 7, and the electric permittivity, see Fig. 8, manifest maxima at intermediate temperatures, and the low-temperature plateaux at most of values of the applied electric field except of the critical one. At the quantum critical value $E = E_c$ the piezoelectric modulus and the electric permittivity grow at low T . On the other hand, the temperature dependence of the elastic modulus, see Fig. 9, manifests minima for the most of values of the applied electric field. At the quantum critical value $E = E_c$ the elastic modulus manifests softening till the lowest temperature.

Thus we see that quantum critical points, characteristic for the quantum spin chain, can manifest themselves in the low-temperature behavior of various characteristics of the system. For this geometry of the electric field (and strain) the most spectacular changes are seen not in the magnetic susceptibility (as it was for $E = E_x$ [19]), but in the behavior of the electric permittivity, piezoelectric modulus, and the elastic modulus in the external electric field.

Analysing the behavior of studied characteristics for nonzero value of J_z at least for $-I \leq J_z \leq I$ in the ground state (using the mentioned above non-perturbative Bethe ansatz results) and at nonzero temperatures (using the Hartree-Fock like approximation [19]), we can conclude that the magnetic, magneto-electric, piezoelectric, and magneto-elastic effects in

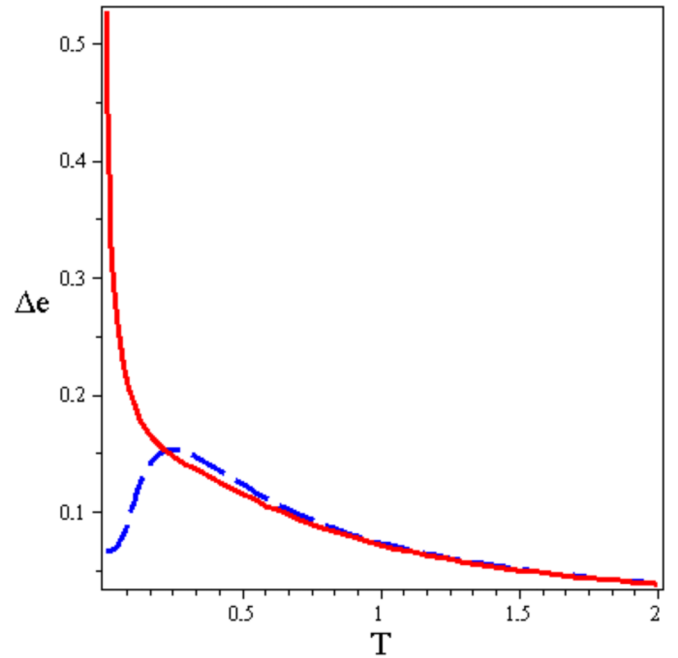


FIG. 7. The temperature dependence of the relative change of the piezoelectric modulus of the spin-1/2 chain for various values of the external electric field E . The parameters of the Hamiltonian are the same as in Fig. 2. $E = 0$ corresponds to the blue-dashed line; $E = E_c = 0.2\sqrt{3}$ is shown with the red-solid line.

the spin chain manifest qualitatively similar to the case $J_z = 0$ behavior.

It is also important to stress that in experiments it is easier to reach the critical values of E than u , because for large

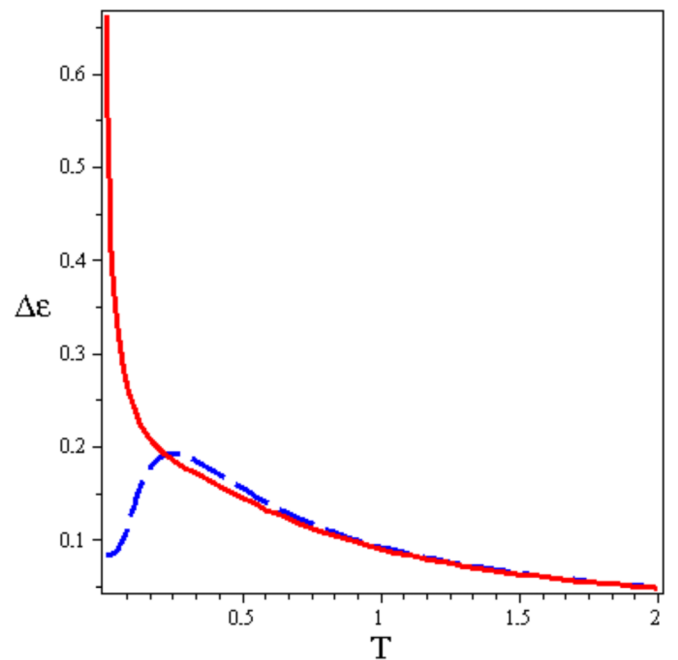


FIG. 8. The temperature dependence of the relative change of the electric permittivity of the spin-1/2 chain for various values of the external electric field E . The parameters of the Hamiltonian and notations are the same as in Fig. 7.

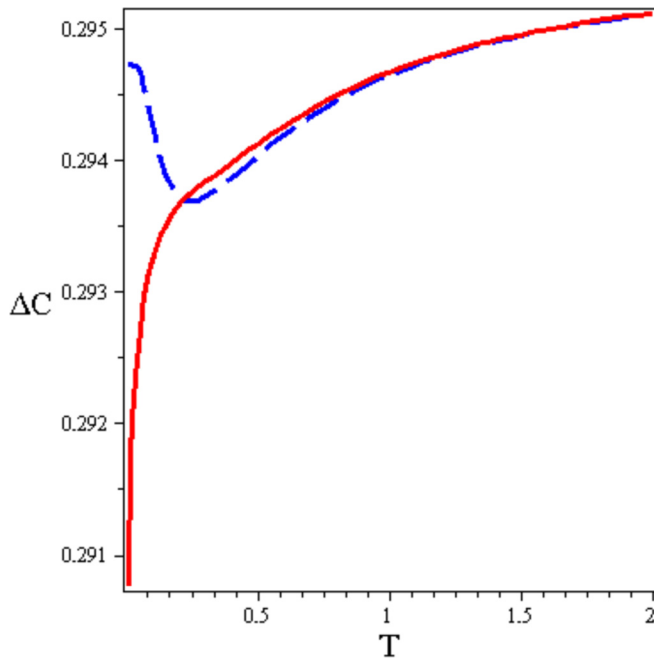


FIG. 9. The temperature dependence of the relative change of the elastic modulus of the spin-1/2 chain for various values of the external electric field E . The parameters of the Hamiltonian and notations are the same as in Fig. 7.

values of strain one can overcome the threshold of the elasticity theory and deal with the plastic deformation, where our theory is not applicable. Unfortunately, we are not aware about data of magneto-electric and magneto-elastic experiments for spin-chain compounds. However, it is possible to estimate the values of the magneto-electric and magneto-elastic coupling constants in real compounds with the electro-magneto-elastic coupling, $a_{1,2}$ and $b_{1,2}$, using, e.g., [21] for the samarium ferrobortate: Their values at low temperature are about $7 \times 10^{-2} \mu\text{C}/\text{m}^2$ and $18 \times 10^{-6} \text{J}/\text{m}^3$, respectively, i.e., $a_{1,2} \gg b_{1,2}$. The critical values of the electric field and strain are determined by the value of the in-plane magnetic anisotropy J . For spin-chain compounds the latter is of order of Δg^2 times the isotropic exchange along the chain [18], where Δg is the difference between the effective in-plane g factors. Such a difference for spin-chain compounds can be of order of 0.01–0.1 [38,39]. For organic spin-chain systems the isotropic exchange is of order of 10 K [40], and for spin-chain crystals can be of order of 100 K [41]. For example, for the spin-chain crystal $6(\text{MAP})\text{CuCl}_2$ the isotropic exchange

parameter along the chain is 110 K, while the in-plane magnetic anisotropy is 0.76 K [41].

VI. SUMMARY

In summary, using analytical quantum theory we have considered the effect of the external electric field, magnetic field, and strain, which reduce the effective symmetry, on the spin chain system coupled to electric and elastic subsystems of the insulating spin-chain crystal. We have shown that the low-temperature behavior of the characteristics of the system, like the magnetic susceptibility, electric permittivity, elastic and piezoelectric module manifest features, governed by the quantum critical points of the spin system. Unlike previously studied case of the electric field and strain, which do not reduce the symmetry, in the present case the effect is determined not only by one component of the spin quadrupole susceptibility, but by two components of the susceptibility, and by the component of the spin quadrupole moment itself. Such a difference yields more complicated ground-state phase diagram with nonlinear quantum critical lines (for the symmetry-preserving strain and electric field such a line is linear). Those critical values can be seen in the special behavior of the temperature dependencies of the mentioned observables. It is different in many aspects from the behavior of similar characteristics of magnetically ordered multiferroics, while some features are similar [21,23,24]. On the other hand, the general features of the temperature and external field behavior of mentioned characteristics are reminiscent of those, observed recently in the rare-earth paramagnet [42]. Such a similarity permits us to conclude that the effects, studied in our paper, have the generic character for magnetic systems with the strong enough coupling between spin, electric, and elastic subsystems. Contrary, the manifestation of quantum critical points and lines are characteristic for quasi-low-dimensional spin systems, and we expect that they can be observed in, e.g., spin-chain compounds, with relatively strong magneto-electro-elastic coupling. We point out that the predicted effects can be very useful in modern microelectronics, due to the possibility to govern, e.g., electric properties by application of the external magnetic field or strain, for the production of switching quantum devices, or in fabrication of ensembles of qubits for quantum computers, which states can be governed by external electro-magnetic fields and strains.

ACKNOWLEDGMENT

The support from the SFB 1143 is acknowledged.

- [1] D. M. Juraschek, P. Narang, and N. A. Spaldin, *Phys. Rev. Research* **2**, 043035 (2020).
- [2] D. M. Juraschek, D. S. Wang, and P. Narang, *Phys. Rev. B* **103**, 094407 (2021).
- [3] S.-W. Cheong and M. Mostovoy, *Nat. Mater.* **6**, 13 (2007).
- [4] Y. Tokura and S. Seki, *Adv. Mater.* **22**, 1554 (2010).
- [5] J. Walowski and M. Münzenberg, *J. Appl. Phys.* **120**, 140901 (2016).
- [6] M. Fechner, A. Sukhov, L. Chotorlishvili, C. Kenel, J. Berakdar, and N. A. Spaldin, *Phys. Rev. Materials* **2**, 064401 (2018).
- [7] V. Atanasov and A. Saxena, *J. Phys.: Condens. Matter* **23**, 175301 (2011).
- [8] K. Roy, S. Bandyopadhyay, and J. Atulasimha, *Appl. Phys. Lett.* **99**, 063108 (2011).
- [9] H. V. Do, T. Lahmer, X. Zhuang, N. Alajlan, H. Nguyen-Xuan, and T. Rabczuk, *Comput. Struct.* **214**, 1 (2019).
- [10] M. Fiebig, *J. Phys. D: Appl. Phys.* **38**, R123 (2005).
- [11] W. Eerenstein, N. D. Mathur, and J. F. Scott, *Nature (London)* **442**, 759 (2006).
- [12] Y. Tokura, *J. Magn. Magn. Mater.* **310**, 1145 (2007).

- [13] K. Wang, J.-M. Liu, and Z. Ren, *Adv. Phys.* **58**, 321 (2009).
- [14] Y. Tokura, S. Seki, and N. Nagaosa, *Rep. Prog. Phys.* **77**, 076501 (2014).
- [15] S. Dong, J.-M. Liu, S.-W. Cheong, and Z. Ren, *Adv. Phys.* **64**, 519 (2015).
- [16] S. Dong, H. Xiang, and E. Dagotto, *Nat. Sci. Rev.* **6**, 629 (2019).
- [17] N. D. Mermin and H. Wagner, *Phys. Rev. Lett.* **17**, 1133 (1966).
- [18] See, e.g., A. A. Zvyagin, *Quantum Theory of One-Dimensional Spin Systems* (Cambridge Scientific Publishers, Cambridge, 2010).
- [19] A. A. Zvyagin, *Phys. Rev. B* **103**, 214410 (2021).
- [20] L. D. Landau and E. M. Lifshitz, *Electrodynamics of Continuous Media* (Pergamon Press, Oxford, 1984).
- [21] T. N. Gaydamak, I. A. Gudim, G. A. Zvyagina, I. V. Bilych, N. G. Burma, K. R. Zhekov, and V. D. Fil, *Phys. Rev. B* **92**, 214428 (2015).
- [22] S. Zherlitsyn, S. Yasin, J. Wosnitza, A. A. Zvyagin, A. V. Andreev, and V. Tsurkan, *Fiz. Nizk. Temp.* **40**, 160 (2014) [*Low Temp. Phys.* **40**, 123 (2014)].
- [23] V. D. Fil, M. P. Kolodyazhnaya, G. A. Zvyagina, I. V. Bilych, and K. R. Zhekov, *Phys. Rev. B* **96**, 180407(R) (2017).
- [24] M. P. Kolodyazhnaya, G. A. Zvyagina, I. V. Bilych, K. R. Zhekov, H. G. Burma, V. D. Fil, and I. A. Gudim, *Fiz. Nizk. Temp.* **44**, 1712 (2018) [*Low Temp. Phys.* **44**, 1341 (2018)].
- [25] L. D. Landau and E. M. Lifshitz, *Elasticity Theory* (Pergamon Press, Oxford, 1984).
- [26] P. Jordan and E. Wigner, *Z. Phys.* **47**, 631 (1928).
- [27] A. A. Zvyagin, *Fiz. Nizk. Temp.* **21**, 825 (1995) [*Low Temp. Phys.* **21**, 636 (1995)].
- [28] W. Thirring, *Ann. Phys.* **3**, 91 (1958).
- [29] S. Coleman, *Phys. Rev. D* **11**, 2088 (1975).
- [30] S. Mandelstam, *Phys. Rev. D* **11**, 3026 (1975).
- [31] V. E. Korepin, *Teor. Mat. Fiz.* **41**, 953 (1979) [*Theor. Math. Phys.* **41**, 953 (1979)].
- [32] H. Bergknoff and H. B. Thacker, *Phys. Rev. Lett.* **42**, 135 (1979).
- [33] H. Bergknoff and H. B. Thacker, *Phys. Rev. D* **19**, 3666 (1979).
- [34] V. E. Korepin, *Commun. Math. Phys.* **76**, 165 (1980).
- [35] A. A. Zvyagin, *Finite Size Effects in Correlated Electron Models: Exact Results* (Imperial College Press, London, 2005).
- [36] A. A. Zvyagin and G. A. Zvyagina, *Phys. Rev. B* **100**, 014416 (2019).
- [37] R. J. Baxter, *Phys. Rev. Lett.* **26**, 834 (1971); *Ann. Phys. (NY)* **70**, 323 (1972).
- [38] See, e.g., E. Frikkee and J. van den Handel, *Physica* **28**, 269 (1962).
- [39] H. Tanaka, T. Ono, S. Maruyama, S. Teraoka, K. Nagata, H. Ohta, S. Okubo, S. Kimura, T. Kambe, H. Nojiri, and M. Motokawa, *J. Phys. Soc. Jpn.* **72** Suppl B, 84 (2003).
- [40] H. Kühne, A. A. Zvyagin, M. Günther, A. P. Reyes, P. L. Kuhns, M. M. Turnbull, C. P. Landee, and H.-H. Klauss, *Phys. Rev. B* **83**, 100407(R) (2011).
- [41] M. Ozerov, A. A. Zvyagin, E. Čížmár, J. Wosnitza, R. Feyerherm, F. Xiao, C. P. Landee, and S. A. Zvyagin, *Phys. Rev. B* **82**, 014416 (2010).
- [42] I. V. Bilych, M. P. Kolodyazhnaya, K. R. Zhekov, G. A. Zvyagina, V. D. Fil, and I. A. Gudim, *Fiz. Nizk. Temp.* **46**, 1092 (2020) [*Low Temp. Phys.* **46**, 923 (2020)].